11th International Conference on Vibration Problems
Z. Dimitrovová *et al.* (eds.)
Lisbon, Portugal, 9-12 September 2013

NONLINEAR FREE VIBRATIONS OF 3D COMPOSITE BEAMS

S. Stoykov*, S. Margenov

Institute of Information and Communication Technologies, Bulgarian Academy of Sciences,
Acad. G. Bonchev str., bl. 25A, 1113 Sofia, Bulgaria

{stoykov, margenov}@parallel.bas.bg

Keywords: Layered beams, Zigzag function, Warping function, Nonlinear normal modes, Bifurcation diagrams.

Abstract. *Geometrically nonlinear free vibrations of composite laminated 3D beams are investigated in the frequency domain by continuation and harmonic balance methods. The beam is modelled by using refined zigzag theory, which contains the kinematics of Timoshenko beam theory and employees continuity of the longitudinal displacement along the thickness of the beam. Zigzag rotational function is used to model the cross sectional distortion due to bending, it is related with piecewise linear functions for each layer, which depend on the material properties and the thickness of the layer. As a result, the transverse shear stress is piecewise constant across the layers' thickness. It is assumed that the cross section rotates as a rigid body, under torsion, and may deform in longitudinal direction due to warping. The warping function is evaluated numerically by solving the Laplace equation with Neumann boundary conditions. The geometric nonlinearity is taken into account by considering Green's nonlinear strain tensor. The equation of motion is derived by the principle of virtual work and discretized into a system of ordinary differential equations by the p-version FEM.*

The derived model of composite laminated 3D beams is validated by generating a fine mesh of three-dimensional finite elements. The resulting large-scale FE system is solved numerically by scalable parallel solvers. A comparison between the derived beam model and the three-dimensional FE model of the natural frequencies is presented.

Nonlinear normal modes are examined, hence the solution is expressed in Fourier series and the resulting nonlinear algebraic system is solved by an arc-length continuation method in the frequency domain. Coupling between modes is investigated, internal resonances are found and the ensuing secondary branches are presented.

1 INTRODUCTION

The use of laminated composite structures has been increased significantly in the last decades in the design of modern engineering applications. Often these structures are modelled like beams vibrating in space, i.e. beams that perform longitudinal and transverse displacements in both principle axes and torsion. The aim of the current paper is to present an accurate model and investigate the dynamical behaviour in the frequency domain of 3D composite beams.

The classical Bernoulli-Euler and Timoshenko beam theories are not appropriate for modelling composite and sandwich beams because they cannot approximate the complex cross sectional behaviour due to axial-bending coupling of the different layers. Improvements of these theories resulted in Equivalent Single Layer (ESL) theories and Discrete Layer Theories (DLT) [1]. In the ESL theories, the number of unknowns is independent of the number of layers but they lead to poor approximation of the shear stresses. In the DLT, the number of unknowns is assumed layer by layer, which leads to sufficiently accurate results. The DLT are more accurate than the ESL theories, but are computationally expensive. The zigzag theories are important subclass of DSL theories, they assume a zigzag distribution of the longitudinal displacement and the number of kinematic variables is independent of the number of layers. The accuracy of the zigzag theories is comparable to the accuracy of the DLT and the computational efficiency is comparable to the ESL theories [2, 3].

In the current work, the beam is modelled by refined zigzag theory [4, 5], which employees continuity of the longitudinal displacement along the thickness of the beam. Piecewise linear functions are defined for each layer, which depend on the material properties and the thickness of the layer. It is assumed that the cross section rotates as a rigid body, under torsion, and may deform in longitudinal direction due to warping [6]. The warping function is evaluated numerically by solving the Laplace equation with Neumann boundary conditions imposing that the traction vectors on the interfaces separating different layers are equal in magnitude and opposite in direction [7]. The equation of motion is derived by the principle of virtual work and discretized into a system of ordinary differential equations by the *p*-version FEM. The unknown vector of generalised coordinates is expressed in Fourier series and the resulting nonlinear algebraic system is solved by an arc-length continuation method in the frequency domain [8].

2 MATHEMATICAL MODEL

The equation of motion of laminated composite beams with rectangular cross sections (Figure 1) is derived in this section. It is based on Timoshenko's theory for bending [9], but includes zigzag functions, which are used to model the cross sectional distortion due to bending [5]. The model assumes that the cross section rotates as a rigid body, but may deform due to warping in the longitudinal direction [6]. The displacements of the beam are expressed by the displacements and rotations on the reference line:

$$\begin{aligned} u(x,y,z,t) &= u_0(x,t) - (y-y_c)\,\phi_z(x,t) + (z-z_c)\,\phi_y(x,t) + \psi(y,z)\,\frac{\partial \theta_x}{\partial x}(x,t) + \\ &\quad + \varphi^{(i)}(z)\chi(x,t) \\ v(x,y,z,t) &= v_0(x,t) + y\cos\big(\theta_x(x,t)\big) - y - z\sin\big(\theta_x(x,t)\big), \\ w(x,y,z,t) &= w_0(x,t) + y\sin\big(\theta_x(x,t)\big) + z\cos\big(\theta_x(x,t)\big) - z, \end{aligned} \tag{1}$$

where u represents the longitudinal displacement, v and w represent the transverse displacements in y and z directions, the subscript 0 denotes the displacements on the reference line, θ_x is the rotation of the cross section about the longitudinal axis x, ϕ_y and ϕ_z denote rotations of

the cross section about axes y and z, respectively, and $\psi(y,z)$ is the warping function. $\chi(x,t)$ is a zigzag rotational function used to model the cross sectional distortion due to bending, it is related with piecewise linear functions for each layer, which depend on the material properties and the thickness of the layer. The piecewise linear functions $\varphi^{(i)}$, proposed in [5] are used in this work. As a result, the transverse shear stress is piecewise constant across the layers' thickness. The point $(y_c,\ z_c)$ denotes the centroid of the cross section, while for the centre of the coordinate system is chosen the twist centre of the cross section. For beams with rectangular cross sections and with symmetric layers with respect to the y axis, these two points coincide with the geometrical centre of the rectangular.

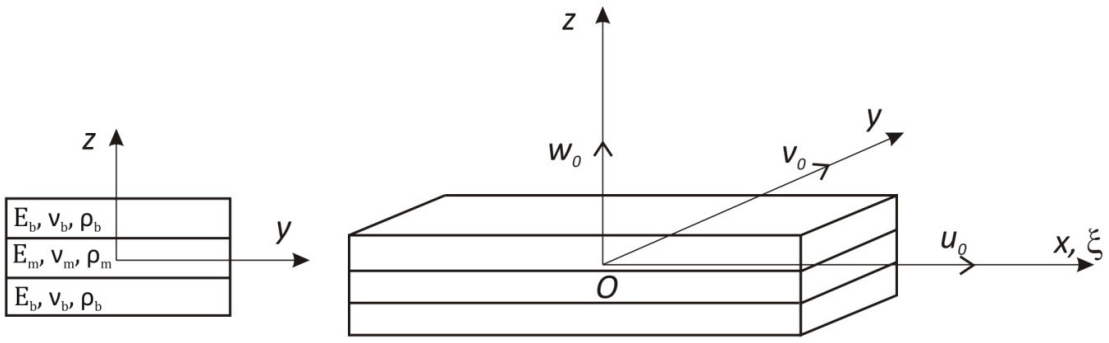

Figure 1: Axes and displacements of layered composite beam.

The warping function is evaluated numerically by solving the Laplace equation with Neumann boundary conditions imposing that the traction vectors on the interfaces separating different layers are equal in magnitude and opposite in direction [6, 7]:

$$\begin{aligned} &\nabla^2\psi = 0 \ \text{ in } \ \Omega = \cup_{i=1}^{\mathrm{M}}\Omega_i \\ &G_i\left(\frac{\partial\psi}{\partial n}\right)_i - G_j\left(\frac{\partial\psi}{\partial n}\right)_j = \left(G_i - G_j\right)\left(z\,n_y - y\,n_z\right) \ \text{ on } \ \Gamma_i, i = 1,\dots,\mathrm{M} \end{aligned} \tag{2}$$

where G_i are the shear modulus of elasticity of regions Ω_i, $i = 1,\dots,\mathrm{M}$. The warping function is obtained preliminarily by finite element method. As a result, the warping and the torsional constants are obtained.

The displacements on the reference line and the rotations of the cross sections are expressed by shape functions and generalized coordinates:

$$\begin{Bmatrix} u_0(\xi,t) \\ v_0(\xi,t) \\ w_0(\xi,t) \\ \theta_x(\xi,t) \\ \phi_y(\xi,t) \\ \phi_z(\xi,t) \\ \chi(\xi,t) \end{Bmatrix} = \begin{bmatrix} \mathbf{N^u}(\xi)^{\mathrm{T}} & \mathbf{0} & \mathbf{0} & \mathbf{0} & \mathbf{0} & \mathbf{0} & \mathbf{0} \\ \mathbf{0} & \mathbf{N^v}(\xi)^{\mathrm{T}} & \mathbf{0} & \mathbf{0} & \mathbf{0} & \mathbf{0} & \mathbf{0} \\ \mathbf{0} & \mathbf{0} & \mathbf{N^w}(\xi)^{\mathrm{T}} & \mathbf{0} & \mathbf{0} & \mathbf{0} & \mathbf{0} \\ \mathbf{0} & \mathbf{0} & \mathbf{0} & \mathbf{N^{\theta_x}}(\xi)^{\mathrm{T}} & \mathbf{0} & \mathbf{0} & \mathbf{0} \\ \mathbf{0} & \mathbf{0} & \mathbf{0} & \mathbf{0} & \mathbf{N^{\phi_y}}(\xi)^{\mathrm{T}} & \mathbf{0} & \mathbf{0} \\ \mathbf{0} & \mathbf{0} & \mathbf{0} & \mathbf{0} & \mathbf{0} & \mathbf{N^{\phi_z}}(\xi)^{\mathrm{T}} & \mathbf{0} \\ \mathbf{0} & \mathbf{0} & \mathbf{0} & \mathbf{0} & \mathbf{0} & \mathbf{0} & \mathbf{N^{\chi}}(\xi)^{\mathrm{T}} \end{bmatrix} \begin{Bmatrix} \mathbf{q_u}(t) \\ \mathbf{q_v}(t) \\ \mathbf{q_w}(t) \\ \mathbf{q_{\theta_x}}(t) \\ \mathbf{q_{\phi_y}}(t) \\ \mathbf{q_{\phi_z}}(t) \\ \mathbf{q_{\chi}}(t) \end{Bmatrix}$$

where $\xi \in$ [-1..1] is the local coordinate.

The shape functions used in the previous works [10, 11] are used here. The shape functions used for the rotations about the transverse axes ϕ_y and ϕ_z are used also for the zigzag rotational function χ.

The strains are derived from Green's strain tensor where the longitudinal displacements of second order are neglected:

$$\varepsilon_x = \frac{\partial u}{\partial x} + \frac{1}{2}\left(\frac{\partial v}{\partial x}\right)^2 + \frac{1}{2}\left(\frac{\partial w}{\partial x}\right)^2,$$
$$\gamma_{zx} = \frac{\partial w}{\partial x} + \frac{\partial u}{\partial z} + \frac{\partial v}{\partial z}\frac{\partial v}{\partial x} + \frac{\partial w}{\partial z}\frac{\partial w}{\partial x}, \tag{4}$$
$$\gamma_{xy} = \frac{\partial u}{\partial y} + \frac{\partial v}{\partial x} + \frac{\partial v}{\partial x}\frac{\partial v}{\partial y} + \frac{\partial w}{\partial x}\frac{\partial w}{\partial y}.$$

The stresses are related with the strains by Hooke's law. A shear correction factor of 5/6 is applied only to the shear stress τ_{xy}, there's no need of shear correction factor to the shear stress τ_{xz} because of the zigzag function [4, 5].

The equation of motion is derived by the principle of virtual work, it is obtained in the following form:

$$\mathbf{M}\,\ddot{\mathbf{q}} + \mathbf{KL}\,\mathbf{q} + \mathbf{KNL}(\mathbf{q})\,\mathbf{q} = \mathbf{0}, \tag{4}$$

where $\mathbf{M}$ is the mass matrix, $\mathbf{KL}$ is the stiffness matrix of constant terms and $\mathbf{KNL}(\mathbf{q})$ is the stiffness matrix which depends linearly and quadraticaly on the vector of generalized coordinates $\mathbf{q}$.

The longitudinal inertia has a small influence in the problem at hand [12] and is neglected; the vector $\mathbf{q_u}(t)$ is eliminated from the equation of motion without neglecting it [11].

Nonlinear normal modes are investigated, hence the solution is assumed to be periodic and it is expressed in Fourier series:

$$\begin{Bmatrix} \mathbf{q_v}(t) \\ \mathbf{q_w}(t) \\ \mathbf{q_{\theta_x}}(t) \\ \mathbf{q_{\phi_y}}(t) \\ \mathbf{q_{\phi_z}}(t) \\ \mathbf{q_\chi}(t) \end{Bmatrix} = \frac{1}{2}\begin{Bmatrix} \mathbf{Q_{v_0}} \\ \mathbf{Q_{w_0}} \\ \mathbf{Q_{\theta_{x_0}}} \\ \mathbf{Q_{\phi_{y_0}}} \\ \mathbf{Q_{\phi_{z_0}}} \\ \mathbf{Q_{\chi_0}} \end{Bmatrix} + \sum_{i=1}^{k} \begin{Bmatrix} \mathbf{Q_{v_i}} \\ \mathbf{Q_{w_i}} \\ \mathbf{Q_{\theta_{x_i}}} \\ \mathbf{Q_{\phi_{y_i}}} \\ \mathbf{Q_{\phi_{z_i}}} \\ \mathbf{Q_{\chi_i}} \end{Bmatrix} \cos(i\omega t) \tag{5}$$

where k is the number of harmonics used in the Fourier series. The time dependent generalized coordinates are replaced by their Fourier expansion (5), inserted in the equation of motion (4) and the harmonic balance method is employed. The resulting algebraic equation of motion in frequency domain has the form:

$$\mathcal{F}(\mathbf{Q}, \omega) \equiv \left(-\omega^2\,\mathbf{M}^{\mathrm{HBM}} + \mathbf{KL}^{\mathrm{HBM}} + \mathbf{KNL}^{\mathrm{HBM}}(\mathbf{Q})\right)\mathbf{Q} = \mathbf{0} \tag{6}$$

where ω is the frequency of vibration and $\mathbf{Q}$ is the vector of unknown coefficients of the harmonics. $\mathbf{M}^{\mathrm{HBM}}$, $\mathbf{KL}^{\mathrm{HBM}}$ and $\mathbf{KNL}^{\mathrm{HBM}}(\mathbf{Q})$ are matrices which result from the matrices from equation (5) due to application of HBM.

The resulting nonlinear algebraic system is solved by an arc-length continuation method [8] in the frequency domain.

3 WARPING FUNCTION FOR COMPOSITE CROSS SECTIONS

In this section the warping function for composite cross sections with different materials is presented and it is compared with the warping function obtained for cross section of one isotropic material, for which there exists an analytical solution. A square cross section is chosen for the comparisons and it is divided by three equal layers. The upper and the bottom layers

are with equal materials and the shear modulus of the middle material is varying. The warping function is presented on Figure 2. The last example corresponds to the warping function of cross section composed of one isotropic material given in [6, 10]. The figure shows how the warping changes when the materials become highly dissimilar. The different colours present the variation of the warping function in positive and negative direction.

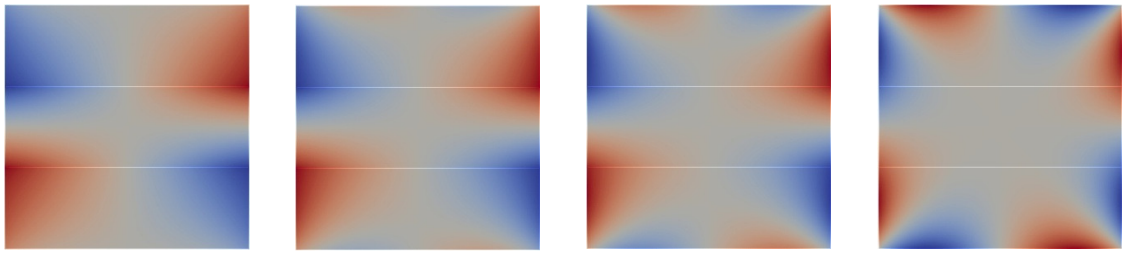

(a) (b) (c) (d)

Figure 2: Warping function for composite cross sections with different stiffness characteristics. $G_b = 1.71\ 10^{10}$ Pa, (a) $G_m = 2.7\ 10^9$ Pa, (b) $G_m = 7.5\ 10^9$ Pa, (c) $G_m = 1.12\ 10^{10}$ Pa, (d) $G_m = 1.71\ 10^{10}$ Pa

4 VALIDATION

First, the proposed 3D beam model is validated in order to verify the numerical computation of the warping function of the composite materials and the inclusion of the zigzag functions. The natural frequencies of two beams, each with three layers, are compared. The beam is clamped-clamped with length 0.58 m, width 0.015 m and thickness 0.009 m (Figure 1). Each of the three layers have equal thicknesses, they are of isotropic materials with different material properties, given in Table 1. The upper and the bottom layers are from equal materials.

Property	Beam 1	Beam 2
E_b	$45.54\ 10^9$ N/m^2	$45.54\ 10^9$ N/m^2
ν_b	0.33	0.33
ρ_b	2040 kg/m^3	2040 kg/m^3
E_m	$7.25\ 10^6$ N/m^2	$7.25\ 10^9$ N/m^2
ν_m	0.45	0.45
ρ_m	1200 kg/m^3	1200 kg/m^3

Table 1: Material properties of beams.

The middle layer of Beam 1 is chosen to be with significantly different elastic properties than the other two layers. The middle layer of the second beam is chosen to be with Young modulus which is closer to the Young modulus of the top and bottom layers.

The FEM software Elmer [13], is used to validate the layered beam. A fine mesh of quadratic tetrahedrons is generated using Gmsh [14]. The mesh has 549614 elements which results into 784233 nodes, each node has three DOF, i.e. the resulting system has more than 2 million DOF. It is solved by parallel computing, using the library Mumps (MUltifrontal Massively Parallel Solver) [15] which is a parallel direct sparse solver. It was verified, by reducing the edges of the tetrahedrons by two, that the results obtained by the large-scale model are converged.

The natural frequencies of both beams are presented in Tables 2 and 3. The importance of the zigzag functions can be seen from Table 2, where the natural frequencies obtained without the zigzag functions differ significantly from the ones obtained with zigzag function and with

three-dimensional finite elements obtained by Elmer. It should be pointed out that the top and bottom layers of both beams are with equal materials and the cross sections are rectangular, thus the cross sections are symmetric with respect to the transverse axes and consequently there is no coupling between both transverse displacements and torsion. Thus, the natural frequencies related with bending in *xy* and with torsion, are not influenced by the zigzag function. The mode shapes associated with each frequency, given in the tables, correspond to the beam model with zigzag function and to the results obtained by Elmer.

Mode	Current model with zigzag function 70 DOF	Current model without zigzag function 60 DOF	Elmer	Mode shape	Difference %
1	344.441	860.801	345.346	Bending xz	0.26
2	824.029	1191.482	822.328	Bending xz	0.21
3	1191.482	2368.020	1192.142	Bending xy	0.06
4	1484.819	3271.031	1489.484	Bending xz	0.31
5	2345.768	4373.871	2352.968	Bending xz	0.31
6	3271.031	4623.787	3265.390	Bending xy	0.17
7	3410.727	6362.327	3421.321	Bending xz	0.31
8	4587.183	7613.815	4470.043	Torsion	2.62
9	4686.677	8814.368	4696.504	Bending xz	0.21
10	6362.327	10437.009	6179.900	Bending xy	2.95

Table 2: First 10 natural frequencies (rad/s) of layered beam with material properties of Beam 1. The difference is between results of the current model with zigzag functions and Elmer.

The natural frequencies of the second beam, i.e. layered beam with materials which have closer elastic properties, are presented in Table 2. The cross sectional distortion due to bending is smaller in this case, due to the similar stiffness characteristic of the materials and the zigzag function has less influence. Nevertheless, its inclusion in the model, is essential for better approximation of the natural frequencies of bending in *xz* plane.

Mode	Current model with zigzag function 70 DOF	Current model without zigzag function 60 DOF	Elmer	Mode shape	Difference %
1	859.835	863.530	861.849	Bending xz	0.23
2	1237.034	1237.034	1240.331	Bending xy	0.27
3	2356.764	2375.768	2357.552	Bending xz	0.03
4	3393.910	3393.910	3398.634	Bending xy	0.14
5	4568.186	4639.884	4576.130	Bending xz	0.17
6	6592.791	6592.791	6610.202	Bending xy	0.26
7	7473.808	7641.749	7473.096	Bending xz	0.01
8	10261.072	10261.072	10160.954	Torsion	0.99
9	10802.859	10802.859	10819.906	Bending xy	0.16
10	11001.814	11360.300	11006.196	Bending xz	0.04

Table 3: First 10 natural frequencies (rad/s) of layered beam with material properties of Beam 2. The difference is between results of the current model with zigzag functions and Elmer.

5 NONLINEAR NORMAL MODES

The nonlinear modes of the layered beam, considering the two different materials given in Table 1, are investigated in this section. The continuation method is started with the linear fundamental natural frequency, i.e. bending in *xz*, with the corresponding eigenvector scaled with small amplitude. Three harmonics are used in the Fourier series in Eq. (5). The first main branch, the bifurcation points and the corresponding secondary branched are shown on Figure 3. The dimensionless amplitude of the first harmonic of the transverse displacement w_0 is used for the plot.

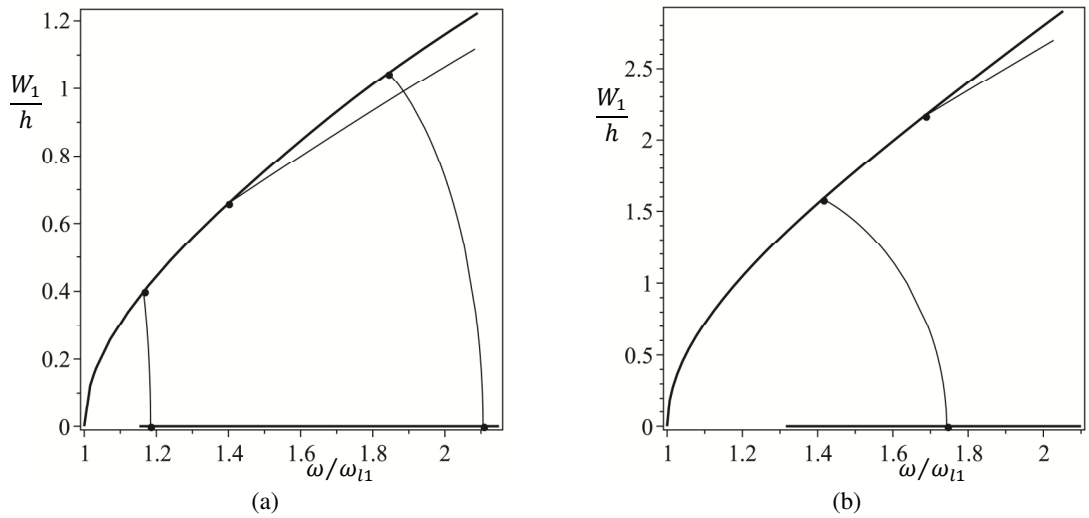

Figure 3: Bifurcation diagrams that start from the first linear mode of bending in *z*, first harmonic. • bifurcation point, ── main branch, — secondary branch. (a) Beam 1, (b) Beam 2, $\xi = 0$, ω_{l1} - fundamental frequency.

Following the main branch of Beam 1 (Figure 3a), a bifurcation point is found for value of the frequency of vibration $\omega/\omega_{l1} \cong 1.16$. At this value, the frequency of vibration becomes one third of the first frequency of bending in *xy* (Table 2). Thus, 1:3 internal resonance exists which couples the first mode of bending in *xz* related with the first harmonic and the first mode of bending in *xy* related with the third harmonic. Due to the nonlinear terms, the third harmonics of the transverse displacements are also excited, as well torsion. The secondary branch goes to another main branch, which vibrates in the *xy* plane, with shape similar to the first mode but related with the third harmonic. The third bifurcation point relates the same modes, but now due to 1:2 internal resonance, i.e. the vibration of the beam, following the secondary branch, continuously transforms from bending in *xz* with shape similar to the first mode and with the first harmonic to bending in *xy* with shape similar to the first mode but with the second harmonic. Due to the symmetry of the cross section, the nonlinearity of the equation of motion on the main branch is cubic, thus only the odd harmonics are excited on the main branch. The second bifurcation point is due to interaction of the bending frequencies in *xz* plane, the vibration remains in the same plane, but even harmonics are also excited.

The first bifurcation point from the main branch of Beam 2 (Figure 3b) also couples both transverse displacements and leads to vibration in space. It appears for value of the frequency of vibration $\omega/\omega_{l1} \cong 1.41$, at which the frequency of vibration becomes one third of the second frequency of bending in *xy*. The bifurcation point is due to 1:3 internal resonance. The secondary branch leads to a second main branch in which the vibration is in *xy* plane, it is with shape similar to the second mode of bending which vibrates with the second harmonic. The second bifurcation point appears at $\omega/\omega_{l1} \cong 1.68$, it is similar to the second bifurcation

point of Beam 1, i.e. the vibration in this secondary branch remains in *xz* plane but involves even harmonics.

The bifurcation diagrams of Figure 3 show that with changes of the material properties of some of the layers, not only the natural frequencies change (Tables 2 and 3), but also the bifurcation points appear at different values, as well, they involve different modes related with different harmonics.

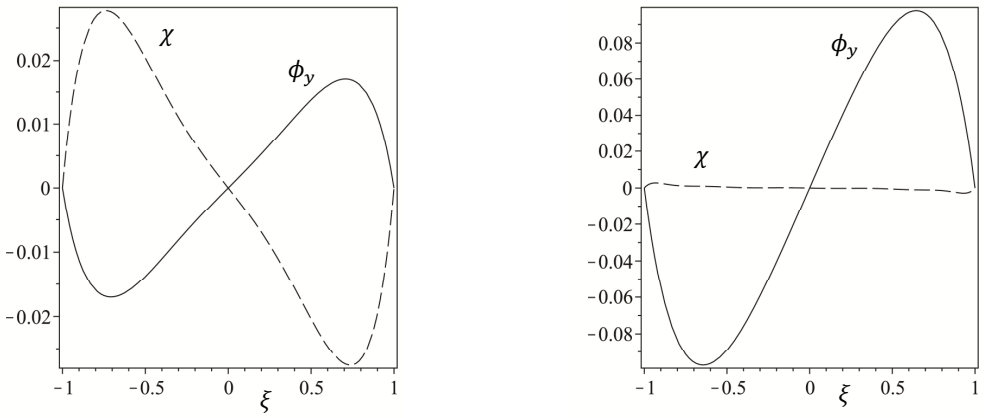

Figure 4: Comparison of rotation about the transverse axis *y* and the zigzag rotational function for a point $\omega/\omega_{l1} \approx 1.6$ from the first main branches from the bifurcation diagrams presented in Figure 3. (a) Beam 1, (b) Beam 2, — ϕ_y, --- χ.

The importance of the zigzag rotational function on the natural frequencies of vibration was shown in Tables 2 and 3. Here is presented its influence on the nonlinear normal modes. for both layered beams. It is compared with the rotation of the cross section about the *y* axis and presented on Figure 4, for a point from the main branch $\omega/\omega_{l1} \approx 1.6$. It can be seen that for the layered beam with highly heterogeneous materials, the amplitude of the zigzag rotational function is essential and even bigger than the amplitude of the rotation of the cross section about the *y* axis. For the layered beam with materials which have similar elastic parameters, the zigzag rotational function exists but its amplitude is much smaller – Figure 4 (b).

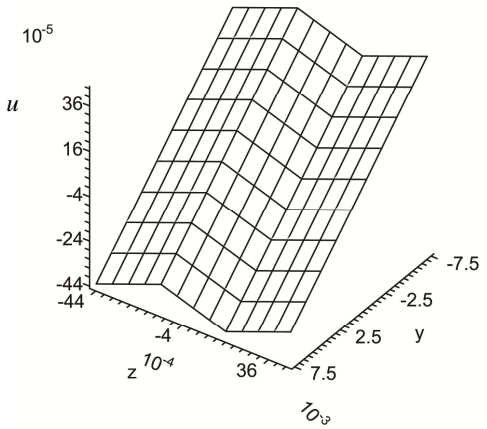

Figure 5: Cross sectional deformation due to bending in space. The influence of both rotations about the transverse axes and the zigzag function, $\omega/\omega_{l1} \approx 2.02$ from the third secondary branch of Beam1, ξ=0.7, *t*=0.

Finally, the deformation of the cross section due to both rotations about the transverse axes and due to the rotational zigzag function is presented in Figure 5 for Beam 1, i.e. for the beam with highly dissimilar materials, for a point from the third secondary branch at $\omega/\omega_{l1} \approx 2.02$. At this branch, the vibration is in space, both rotations ϕ_y and ϕ_z are excited as well χ. In the secondary branch, torsion is also excited, due to the bending-torsion coupling due to the geometrically nonlinear terms, thus the cross section deforms also due to warping, which is not included in Figure 5.

6 CONCLUSION

Nonlinear free vibrations of composite layered 3D beams were investigated in this work. The equation of motion was derived by the principle of virtual work and the *p*-version FEM. The Timoshenko's theory for bending was assumed and additional zigzag rotational function was added, which presents the longitudinal distortion of the layers due to bending, it was expressed with piecewise linear functions for each layer, which depend on the material properties and the thickness of the layer. The warping function was obtained numerically, additional boundary conditions were imposed between the layers, i.e. that the traction vectors on the interfaces separating different materials are equal in magnitude and opposite in direction. The vector of generalized coordinates was expressed by Fourier series and replaced in the equation of motion. The resulting algebraic nonlinear system was solved by an arc-length continuation method.

The 3D composite beam model was validated by comparing the natural frequencies of equivalent beam structure with three-dimensional finite elements. It was shown that the reduced model gives results in agreement with the large-scale model. The importance of the rotational zigzag function, for the cases of layered beams with highly dissimilar materials, was pointed out.

The bifurcation diagrams of layered 3D beams were presented, two cases were considered: a beam with material properties of the middle layer which are significantly different than the material properties of the top and bottom layers and with a beam whose material properties of the middle layer are closer to the ones of the top and bottom layers. Several bifurcation points were found and the corresponding secondary branches were described. The vibration of the beam may lead from motion in one plane into motion in space due to interaction of both transverse displacements. It was shown that changing the material properties of some of the layers, change also the interaction between the modes, i.e. some bifurcation points does not appear while new interactions appear.

ACKNOWLEDGEMENT

The research work carried out in the paper is supported by the project AComIn "Advanced Computing for Innovation", grant 316087, funded by the FP7 Capacity Programme (Research Potential of Convergence Regions) and Bulgarian NSF Grant DCVP 02/1.

REFERENCES

[1] E. Carrera, C_z^0 requirements – models for the two dimensional analysis of multilayered structures, *Composite Structures*, **37**, 373-383, 1997.

[2] E. Carrera, Historical review of zig-zag theories for multilayered plates and shells, *Applied Mechanics Reviews*, **56**, 287-307, 2003.

[3] S. Kapuria, P. Dumir, A. Ahmed, An efficient higher order zigzag theory for composite and sandwich beams subjected to thermal loading, *Solids and Structures*, **40**, 6613-6631, 2003.

[4] A. Tessler, M. Di Sciuva, M. Gherlone, A refined zigzag beam theory for composite and sandwich beams, *Journal of Composite Materials*, **43**, 1051-1081.

[5] M. Gherlone, A. Tessler, M. Di Sciuva, C^0 beam elements based on the refined zigzag theory for multilayered composite laminates, *Composite Structures*, **93**, 2882-2894, 2011.

[6] I. Sokolnikoff, *Mathematical theory of elasticity*, McGraw-Hil, New York, 1956.

[7] E. Sapountzakis, Torsional vibrations of composite bars by BEM, *Composite Structures*, **70**, 229-239, 2005.

[8] R. De Borst, M. Crisfield, J. Remmers, C. Verhoosel, *Non-linear finite element analysis of solids and structures*, John Wiley & Sons, 2012.

[9] C. Wang, J. Reddy, K. Lee, *Shear deformable beams and plates*, Elsevier, Oxford, 2000.

[10] S. Stoykov, P. Ribeiro, Nonlinear forced vibrations and static deformations of 3D beams with rectangular cross section: The influence of warping, shear deformation and longitudinal displacements, *International Journal of Mechanical Sciences*, **52**, 1505-1521, 2010.

[11] S. Stoykov, P. Ribeiro, Nonlinear free vibrations of beams in space due to internal resonance, *Journal of Sound and Vibration*, **330**, 4574-4595, 2011.

[12] P. Ribeiro, Hierarchical finite element analyses of geometrically non-linear vibration of beams and plane frames, *Journal of Sound and Vibration*, **246**, 225-244, 2001.

[13] Elmer web site: www.csc.fi/elmer (last time visited 24/05/2013).

[14] C. Geuzaine, J.-F. Remacle, Gmsh: a three-dimensional finite element mesh generator with built-in pre- and post-processing facilities, *International Journal for Numerical Methods in Engineering*, **79**, 1309-1331, 2009.

[15] P. Amestoy, A. Guermouche, J. L'Excellent, S. Pralet, Hybrid scheduling for the parallel solution of linear systems, *Parallel Computing*, **32**, 136-156, 2006.